

# Quantitative Characterization of Interdiffusion at the Resin–Resin and Resin–Prepreg Interphases of Epoxy Systems Processed by Model SQ-RTM

W. Ballout,<sup>1</sup> B. Coulon,<sup>1</sup> Y.-A. Janssens,<sup>2</sup> P. Van Velthem,<sup>1</sup> M. Sclavons,<sup>1</sup> D. Magnin,<sup>1</sup> T. Pardoën,<sup>2</sup> C. Bailly<sup>1</sup>

<sup>1</sup>Institute of Condensed Matter and Nanosciences-Bio & Soft Matter (IMCN/BSMA)-Université Catholique De Louvain, Louvain-la-Neuve, 1348, Belgium

<sup>2</sup>Institute of Mechanics, Materials and Civil Engineering (iMMC), Université Catholique De Louvain, Louvain-la-Neuve 1348, Belgium

**The interdiffusion between a low and a high viscosity epoxy resin was studied on model systems representing the novel composite manufacturing process called “Same Qualified-Resin Transfer Molding” (SQ-RTM). Neat resin model systems were first characterized after curing by Raman spectroscopy, energy dispersive X-ray microscopy, and nano-indentation, all methods reveal an interdiffusion distance of about 700–900  $\mu\text{m}$ . Transmission electron microscopy further revealed a complex morphological gradient structure in the interdiffusion zone. The interdiffusion distance was about 800  $\mu\text{m}$  in the absence of carbon fibers, reducing down to 500  $\mu\text{m}$  when the viscous resin was replaced by the corresponding prepreg, due to the geometrical constraints imposed by the fibers. Moreover, some asymmetry was observed in the interdiffusion profile because of the viscosity difference between the resins. The results obtained on the model systems were found to match very well the interdiffusion profiles generated in real SQ-RTM composites processed with the same combination of resins. POLYM. ENG. SCI., 00:000–000, 2016. © 2016 Society of Plastics Engineers**

## INTRODUCTION

The use of composite materials based on carbon fabric-reinforced thermoset resins in structural aircraft applications keeps expanding because of the unique combination of mechanical properties, low density, and high thermal as well as chemical resistance. However classical processing methods, such as wet layup or autoclave curing of prepregged fabrics (prepregs) suffer from significant cost issues, both direct due to slow and labor-intensive processes and indirect related to surface finish issues and difficulties in parts integration.

Out-of-autoclave technologies enabling complex shapes with tight tolerances as well as high surface finish, in particular Resin Transfer Molding (RTM), tend to be preferred over autoclave technology as they reduce manufacturing and assembly costs [1]. RTM allows shorter cycle times and excellent dimensional control of complex structural composite parts. Unlike autoclave technologies which use prepregs, the RTM process involves the injection of a low viscosity resin in a closed mold where a dry fabric layup has previously been positioned. However, RTM

suffers from several limitations as well: (i) The pore-free filling of the dry fabric by the resin may be problematic; (ii) the resin injection stage may induce unwanted displacement of the fibers in the mold; (iii) The dry fabric may filter immiscible additives present in the resin.

Considering the RTM and autoclave limitations, an innovative manufacturing process combining the advantages of both, called Same Qualified-Resin Transfer Molding (SQ-RTM) process, has recently been introduced [2, 3]. SQ-RTM is similar to RTM but instead of a dry fabrics placed in the mold, prepregs are used. The challenge with this approach is to generate the adequate pressure within the mold to consolidate the prepregs and to avoid the generation of porosity from residual gases. Hence, an additional resin, in principle identical to the prepreg resin (hence the name “same qualified”) is injected through cavities strategically positioned around the perimeter of the mold in order to apply a sufficient by large hydrostatic pressure during the curing stage (Fig. 1). As the tool is exactly sized for the dimensions of the layup, the additional resin does not pool or produce resin-rich areas but only creates a thin layer along continuous external surfaces. SQ-RTM allows to manufacture composite panels with tight tolerances as well as high surface finish, without the need of post-processing or machining operations. Because of its significant advantages, SQRTM is likely to replace, at least partially, not only autoclave composite manufacturing but also well established out of autoclave technologies, such as RTM.

Nevertheless, resins used in prepregs are often too viscous to serve as pressurizing medium in SQ-RTM. Another injection resin with a lower viscosity must thus be selected. The use of two different resins requires a strict control of their respective curing kinetics to ensure that the injection resin gels after the prepregs, otherwise, the pressure will not be effectively applied on the layup once the injected resin has gelled. The two resins can interdiffuse before gelling [4, 5]. In some cases, the resulting interphase does not affect or is even beneficial to mechanical performance [4]. If the injected resin is identical to the one used in the prepreg, their interfacial mixing has no significant influence on the final properties of the composite. However, this cannot be construed as the general situation. If the prepreg and the injection resin are significantly different, it is essential to analyze their intermingling and to characterize the resulting interphase from composition, morphology, and mechanical response. The objective is to understand the overall impact on the composite properties based on the local characteristics and to determine if there is an absolute need to machine away the outer layer. In realistic cases where a tight carbon fabric prepreg based on a high viscosity resin is pressurized by a relatively

Correspondence to: W. Ballout; e-mail: wael.ballout@uclouvain.be  
Contract grant sponsor: Wallonia region in the frame of “Efficient Composite Technologies for Aircraft Components.”  
DOI 10.1002/pen.24338  
Published online in Wiley Online Library (wileyonlinelibrary.com).  
© 2016 Society of Plastics Engineers

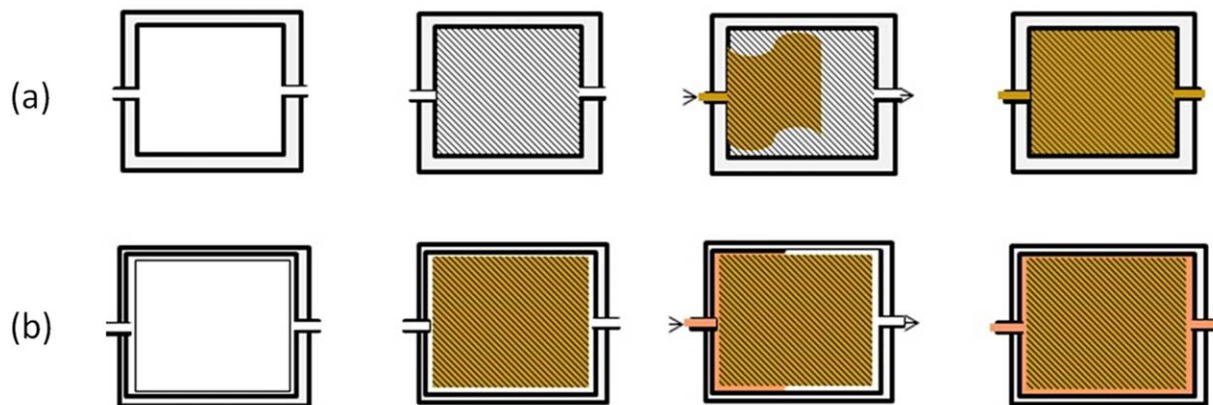


FIG. 1. Comparison between (a) RTM process and (b) The SQ-RTM process; in RTM, the dry preform is impregnated by the resin precursors in the mold under pressure whereas in SQ-RTM, a preimpregnated fabrics are compacted in the mold under pressure by the injection resin. [Color figure can be viewed in the online issue, which is available at [wileyonlinelibrary.com](http://wileyonlinelibrary.com).]

very low viscosity injection resin, the convective motion of the injection resin toward the prepreg resin can be neglected during the entire process as will be confirmed in the results section. Hence, the key phenomenon to consider in order to understand the structure and properties of the interfacial area is the molecular interdiffusion during the curing stage after the mold has been filled and pressurized. To our knowledge no study has reported an in depth characterization of the interdiffusion between two different resins occurring in a SQ-RTM process or any analogous process. In particular no quantitative measurement or analysis of the characteristics of the transition zone is described in the literature. The present investigation aims at filling this gap and provides important insights in the context of the development of the SQ-RTM process. More precisely, the interdiffusion profile at the interphase between two resins will be determined both in the presence and absence of a carbon fiber fabric. Two different types of simplified systems mimicking either resin–resin or resin–prepreg interphases used in SQ-RTM have been produced. SQ-RTM resins, i.e. Hexcel 8552 widely used in prepregs and a developmental injection resin, hereafter named “alpha resin” have been used. The samples have been crosslinked under the same pressure and temperature cycle as the one applied during SQ-RTM in a controlled pressurized oven.

The resin–resin interphase has first been characterized in order to quantify the size of the interdiffusion zone by Raman spectroscopy with the help of chemometrics and scanning electron microscopy (SEM) coupled with energy dispersive X-ray spectrometry (EDX). Moreover, gradient morphologies around the interphase zone have been studied by transmission electron microscopy (TEM). The local mechanical properties and, more specifically, the variation of the elastic modulus have been determined by nano-indentation. The resin–prepreg interphase has also been investigated and compared with the corresponding resin–resin interphase. Finally, a comparison with a real SQ-RTM composite based on the same resin combination has been performed.

## EXPERIMENTAL METHODS

### Materials

The 8552 epoxy resin and 8552 AS4 Tape prepreg produced by Hexcel and qualified for aeronautical applications are used to

prepare the model systems without and with fibers, respectively. The low viscous injection resin used for both model systems, noted “alpha resin” below, is still under development by Hexcel. This alpha resin is composed of epoxies and a curing agent containing chlorine groups as well as some spherical nanoparticles giving a pink color and hence facilitates its visualization. The characteristics and chemical structures of the resins and the prepregs are listed in Table 1 [6–10]. The 8552 resin contains 20% polyethersulfone (PES), which acts as toughener.

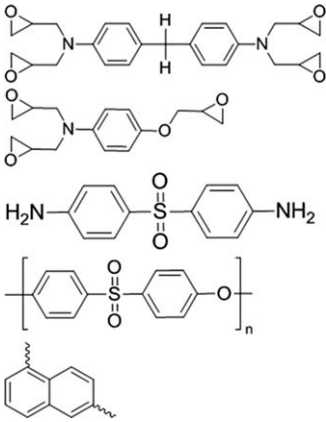
### Samples Preparation

The curing cycle for all the samples is based on both pressure and temperature conditions applied in industry for the production of composite panels based on the 8552 prepregs. The pressure is set to 7 bars while the temperature is first fixed to 80°C for 10 min and then increased using a heating ramp of 2.5°C/min in order to reach 180°C. This final temperature is maintained for 120 min.

A composite panel is manufactured using the SQ-RTM process with the help of a Radius electrical injection system (6000 cc). The panel consisted of 8 layers of 8552 prepreg having 490 mm × 490 mm in size with a quasi-isotropic configuration [ $\pm 45^\circ/(0^\circ/90^\circ)$ ]. The injection resin used to pressurize the prepregs is the alpha resin. After complete filling at 100 mL/min, a dwell pressure of 7 bars is maintained in the mold. The curing cycle involved an isothermal step at 80°C for 10 min (injection time of the alpha resin) followed by a 2.5°C/min ramp from 80°C to 180°C. This temperature is held for 120 min before cooling.

**Calibration Samples.** In addition to the two types of model systems considered for the interdiffusion study, homogenous blends of the 8552 resin/alpha resin are produced over the entire range of compositions (100/0, 90/10, 75/25, 50/50, 25/75, 10/90, 0/100, wt%) in order to generate calibration models used for the chemometrics interpretation of the Raman measurements. The homogenization is performed manually in an aluminum cup at 80°C. Each sample is then placed in an aluminum DSC (differential scanning calorimetry) pan and cured in the oven of a high

TABLE 1. Characteristics and chemical formula of the resins as well as the prepreg fabric.

	8552 resin	8552/AS4 (prepreg)	Alpha resin
Epoxy component	TGMDA, TGAP	TGMDA, TGAP	Naphthalene backbone
Curing agent	DDS	DDS	Chlorine groups
Thermoplastic	PES (20%)	PES (6%)	
Carbon fiber		UD (65%)	
Viscosity (Pa s)	120.8 at 80°C 25.1 at 100°C 7.8 at 120°C 4 at 140°C		0.4 at 80°C 0.15 at 100°C 0.07 at 120°C 0.035 at 140°C
Gel time (min)	141 at 120°C 63 at 140°C		440 at 120°C 193 at 140°C
Annotations:			
TGMDA: Tetraglycidyl methylenedianiline			
TGAP: Triglycidyl- <i>p</i> -aminophenol			
DDS: 3,3 or 4,4 Diaminodiphenylsulfone			
PES: Polyethersulfone			
Naphthalene backbone			
UD: UniDirectionnal			
			

pressure-differential scanning calorimetry (HP-DSC) from Mettler Toledo using the curing cycle described below.

**Model Systems.** The model system without fibers (called “Model System 1”), composed of pure resins only, is obtained by covering a 50 mg 8552 resin layer with a 50 mg alpha resin layer in a 100  $\mu$ L aluminum DSC pan. The pans are sealed and pierced at their top and finally placed in the oven of the HP-DSC. A schematic view of this system is presented in Fig. 2a. The model system with fibers (called model system 2) is

produced in three consecutive steps: (i) prepreg layers preparation, (ii) sample preparation followed by (iii) curing of the sample. The prepreg layers are first conditioned using a vacuum bag in order to avoid the presence of porosity in the sample. The prepreg layer is composed of a carbon fiber pile-up consisting of eight plies positioned in a quasi-isotropic configuration [ $\pm 45^\circ/(0^\circ/90^\circ)$ ].

The curing of the sample takes place in an individual, homemade open mold. A schematic view of the cross-section of the mold containing a “Model System 2” sample is presented in

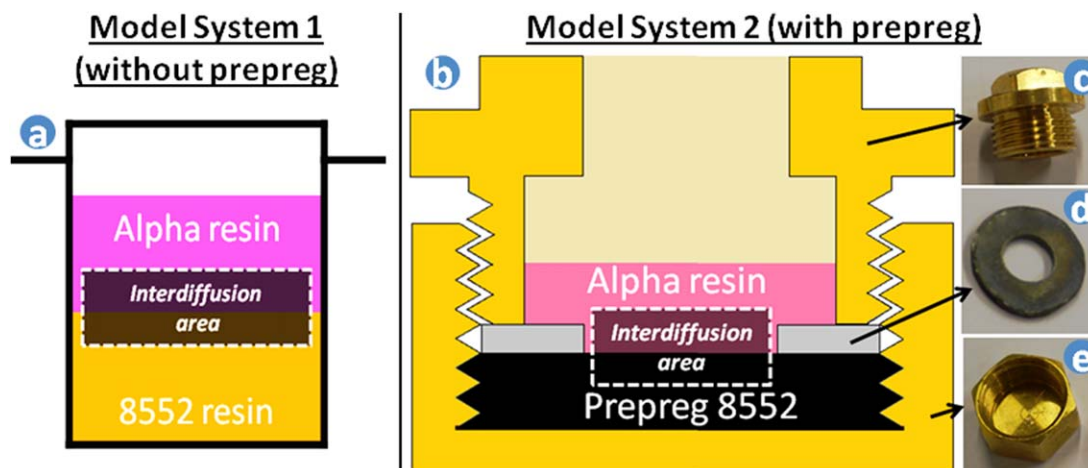


FIG. 2. (a) Schematic view of the DSC pan cross-section containing the resin/resin model system; (b) schematic view of the mold cross-section containing the resin/prepreg model system; (c–e) photos of the mold elements: the pierced 3/8' brass plug (c), the metallic washer (d), and the 3/8' brass compression cap (e). [Color figure can be viewed in the online issue, which is available at [wileyonlinelibrary.com](http://wileyonlinelibrary.com).]

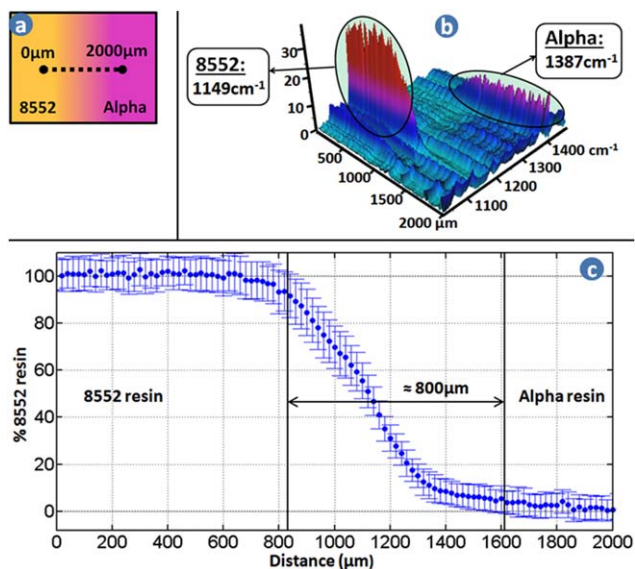


FIG. 3. (a) Schematic representation of the analyzed polished surface of a cured sample; (b) three-dimensional representation of the Raman spectra from the Raman mapping performed every 20  $\mu\text{m}$  along a 2000  $\mu\text{m}$  dotted line on both sides of the interphase and perpendicularly to it; (c) sulfone groups concentration profile of 8552 resin with the standard error at each point calculated from the chemometrics quantification model. [Color figure can be viewed in the online issue, which is available at [wileyonlinelibrary.com](http://wileyonlinelibrary.com).]

Fig. 2b and pictures showing the different assembling elements are given in Fig. 2c–e. In order to avoid any potential interaction during the curing process between the metallic surfaces from the different parts of the mold and the epoxy resin, all surfaces are coated with a release agent (WaterShield<sup>TM</sup>, ZYVAX). The prepreg layer is inserted at the bottom of a compression cap (e) and is covered by a metallic washer (d). This assembly is then compacted by screwing a pierced plug (c) in the cap before introducing 300 mg of alpha resin at the center of the washer.

Curing takes place in a 25 mL Parr pressure vessel (Parr Instrument Company) connected to a temperature regulator (Omron E5CN) and a “5866 Series” Brooks Pressure Controller.

#### Interphase Characterization Methods

The cured samples are cut so as to give access to the cross-section perpendicular to the interphase, see Fig. 2a and b. Each half-sample is next embedded in an EpoFix epoxy resin before the pre-polishing step involving the successive use of finer grades of abrasive paper followed by polishing of the cross-sectional area (mirror finish obtained with a succession of finer particle sizes: 9->3->1  $\mu\text{m}$  diamond polishing).

**Raman Spectroscopy Coupled With Chemometrics.** The measurements with a spatial resolution of 1  $\mu\text{m}$  are performed by Raman spectroscopy using a DXR SmartRaman spectrometer from Thermo Scientific operating in the microscopic mode with a 2048 pixel charge-coupled device detector and equipped with a confocal microscope (Olympus TH4-200). The pinhole aperture is set to 50  $\mu\text{m}$  and a  $\times 50$  magnification objective is used, resulting in the analysis of a spot diameter of 1.27  $\mu\text{m}$ . In order to determine the concentration profile at the interphase between

the two resins, a Raman mapping (measurements taken every 20  $\mu\text{m}$ ) is performed over a distance of 2 mm perpendicularly to the interphase. For each spectrum, the acquisition window ranges from 1485  $\text{cm}^{-1}$  to 1025  $\text{cm}^{-1}$ . The laser, with an incident wavelength of 780 nm and a power of 14 mW, is focused perpendicularly to the sample surface. The recorded spectra are the average of five individual spectra, the acquisition of each spectrum takes 60 s and is performed after 5 min of photo-bleaching in order to reduce both the background noise and the fluorescence.

The 8552 resin concentration is determined using a quantification model based on chemometrics. This model is generated by treating the Raman spectra of the calibration samples with the Unscrambler software. Automatic pretreatments such as smoothing, baseline correction (Multiplicative Signal Correction “MSC”), and the use of a Partial Least Squares (PLS) technique are applied to the spectra [11–16].

#### X-Ray Spectrometry Coupled With Scanning Electronic Microscopy.

Specimens for analysis are mounted on stubs and coated with an 8 nm chromium layer (Cressington sputter 208HR). SEM and X-ray spectrometry coupled with scanning electronic microscopy (SEM-EDX) analyses are performed on polished surfaces using a JEOL FEG SEM 7600F equipped with an EDX system (Jeol JSM2300 with a resolution < 129 eV) operating at 15 keV with a working distance of 8 mm. The acquisition time for the chemical spectra is 300 s with a probe current of 1 nA. The resolution of the EDX is about 0.5  $\mu\text{m}$  [17].

The quantitative analysis of the atomic elements is performed with the integrated Analysis Station software of the instrument. A two-step analysis procedure is applied in order to produce quantitative results for the elemental profiles over the entire cross-sections: (i) The bremsstrahlung is subtracted with the classical “Top Hat Filter” method [18, 19] and (ii) The area under each atomic peak is quantified by the  $\varphi$  ( $\rho z$ ) model [20–22].

**Transmission Electron Microscopy.** The interfacial morphology gradient is characterized by TEM observations. The specimens are extracted from the original samples by cutting, transversally to the interphase, layers with a thickness of about 95 nm. The cutting is performed with a Reichert Microtome using a Histo-diamond knife (angle of 45°) from Diatome (Switzerland) at room temperature. The ultrathin sections are subsequently collected on a 300 mesh copper grid and observed with a LEO 922 (Zeiss) transmission electron microscope operating at 200 kV.

**Nano-Indentation.** The indentation on polished samples is performed with a G200 nano-indenter by Agilent Technologies in CSM (Continuous Stiffness Mode) [23] at room temperature. A flat punch tip [24] with a diameter of 23.65  $\mu\text{m}$  is used. The final indentation depth “ $h$ ” is set equal to 3  $\mu\text{m}$ . The CSM frequency and the applied oscillation are equal to 1 Hz and  $\pm 50$  nm, respectively. The spacing between each indent is 100  $\mu\text{m}$ , corresponding to more than three times the tip diameter in order to avoid the influence of the plastically deformed zones from the neighboring indents. The linescan technique developed by Gwynne et al. [25] is used with 5 sets of 18 indents to cover a wide area across the interphase.

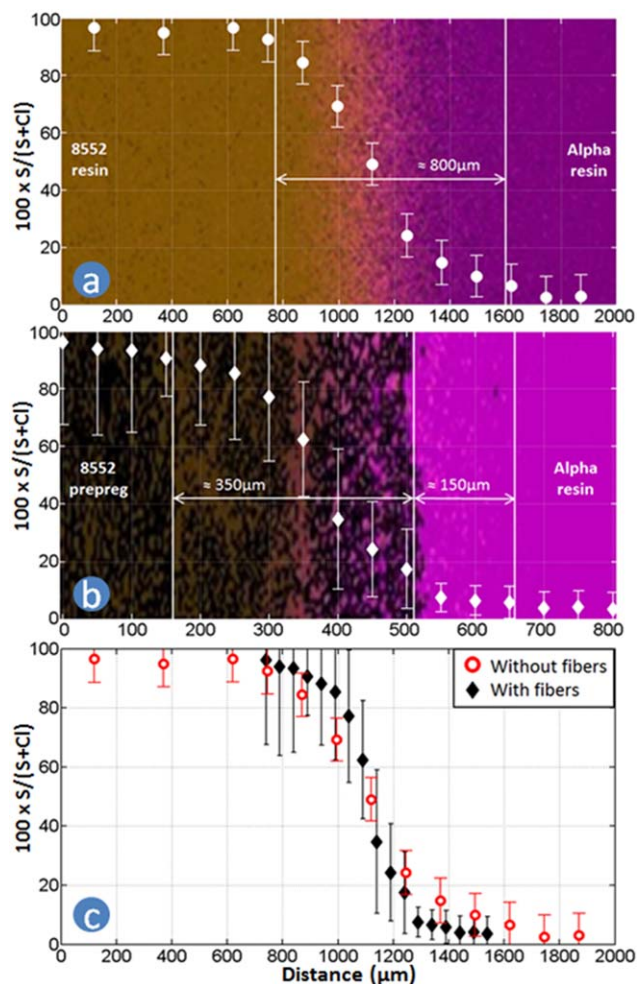


FIG. 4. (a) and (b) sulfur (yellow) and chlorine (purple) SEM-EDX maps of the interphase, for model systems without and with carbon fibers respectively, with their associated interdiffusion profile, (c) concentration of sulfur from 8552 resin with its standard error at the interphase in the presence and absence of carbon fibers. [Color figure can be viewed in the online issue, which is available at [wileyonlinelibrary.com](http://wileyonlinelibrary.com).]

## RESULTS

The interdiffusion profile of the model systems without fibers (Model System 1) is determined using Raman spectroscopy by following the evolution of the spectra in the interfacial region. Because the presence of carbon fibers would completely saturate the signal and could even lead to the burning of the sample, Model System 2 comprising carbon fibers is not used for the characterization by Raman spectroscopy. Similar to the evaluation of the local thermoplastic content in epoxy resin-polyethersulfone blends [12, 26], Raman spectroscopy is exploited to determine the concentration of sulfone groups from diaminodiphenylsulfone (DDS) and PES present in the cured 8552 epoxy resin. The sulfone groups are characterized by an intense Raman spectral band centered at  $1149\text{ cm}^{-1}$  due to their symmetric stretching vibration. The concentration of the cured alpha resin could also be followed thanks to the presence in its Raman spectrum of a strong characteristic band at  $1387\text{ cm}^{-1}$  due to the ring vibration of di-substituted naphthalene groups. The Raman spectra of both pure cured resins are shown in Fig.

3b. The two distinguishable peaks constitute tracers for the 8552 and alpha resins.

Chemometrics is used in this study as a powerful alternative to classical band-specific treatment of the spectra in order to quantify the distribution of the two resins in the interdiffusion zone. Indeed, the calibration procedure coupled with multivariate analysis of the spectra leads to improved accuracy for the prediction of the local sulfone and naphthalene concentrations since confidence intervals can be defined. The methodology used to create, calibrate, and validate the chemometrics model is the same as the one described in Refs. 11–16. Figure 3a gives a schematic representation of the analyzed pre-polished surface of a cured sample. The Raman mapping is performed over a total distance of  $2000\text{ }\mu\text{m}$  along the dotted line on both sides of the interphase and perpendicularly to it. A three-dimensional representation of the Raman spectra from the mapping is shown in Fig. 3b. Qualitatively, the interdiffusion distance corresponds to the region of the decreasing sulfone peak and the increasing naphthalene peak.

The 8552 resin concentration profile resulting from the chemometrics quantification model is presented in Fig. 3c. The standard error, calculated from all the Raman spectra of the mapping, is also represented for each point of the profile. An interdiffusion distance of about  $800\text{ }\mu\text{m}$  can be estimated from the profile when adding one standard deviation to the estimated concentrations.

The Model Systems 1 and 2 (without and with carbon fibers) are also characterized by SEM-EDX. The analysis of tracer atoms, e.g. sulfur, to follow a resin concentration profile by SEM-EDX has already been described in the literature for a combined infusion-prepreg system [27]. An EDX analysis is performed across the interphase by tracing the sulfur element from the 8552 prepreg and the chlorine element from the alpha resin. Similar to the methodology used for Raman, a mapping is performed perpendicularly across the interphase. The relative concentrations of carbon, sulfur, and chlorine atoms with their standard error are calculated as the average along a fictive line parallel to interphase (i.e., parallel to the  $Y$  axis of the SEM-EDX pictures in Fig. 4) on a given area of the polished samples. The 8552 resin mass concentration is defined as  $[100 \times \text{Sulfur} / (\text{Sulfur} + \text{Chlorine})]$ .

Figure 4a and b shows color maps indicating the sulfur (yellow) and chlorine (purple) concentration as observed by SEM-EDX. These color maps provide an alternative determination of the interdiffusion profiles in the absence (a) and presence (b) of carbon fibers, respectively, with comparison as shown in Fig. 4c. The interdiffusion distance is estimated from the concentrations (with one standard deviation added) in the 0–100% range for Model System 1 without carbon fibers and between 0 and 90% for Model System 2 with carbon fibers. The choice of the arbitrary upper limit of 90% is justified by the reduced accuracy of the measurements in the presence of carbon fibers. An interdiffusion distance of  $800\text{ }\mu\text{m}$  could be estimated for the model system without carbon fibers similar to the Raman spectroscopy results. This distance is reduced down to  $500\text{ }\mu\text{m}$  in the presence of carbon fibers and is of the same order of magnitude as the interdiffusion distance described in combined infusion-prepreg systems [27]. The lower diffusion distance is a consequence of the complex diffusion path involving meandering induced by the presence of the fabric, with a dependence on its

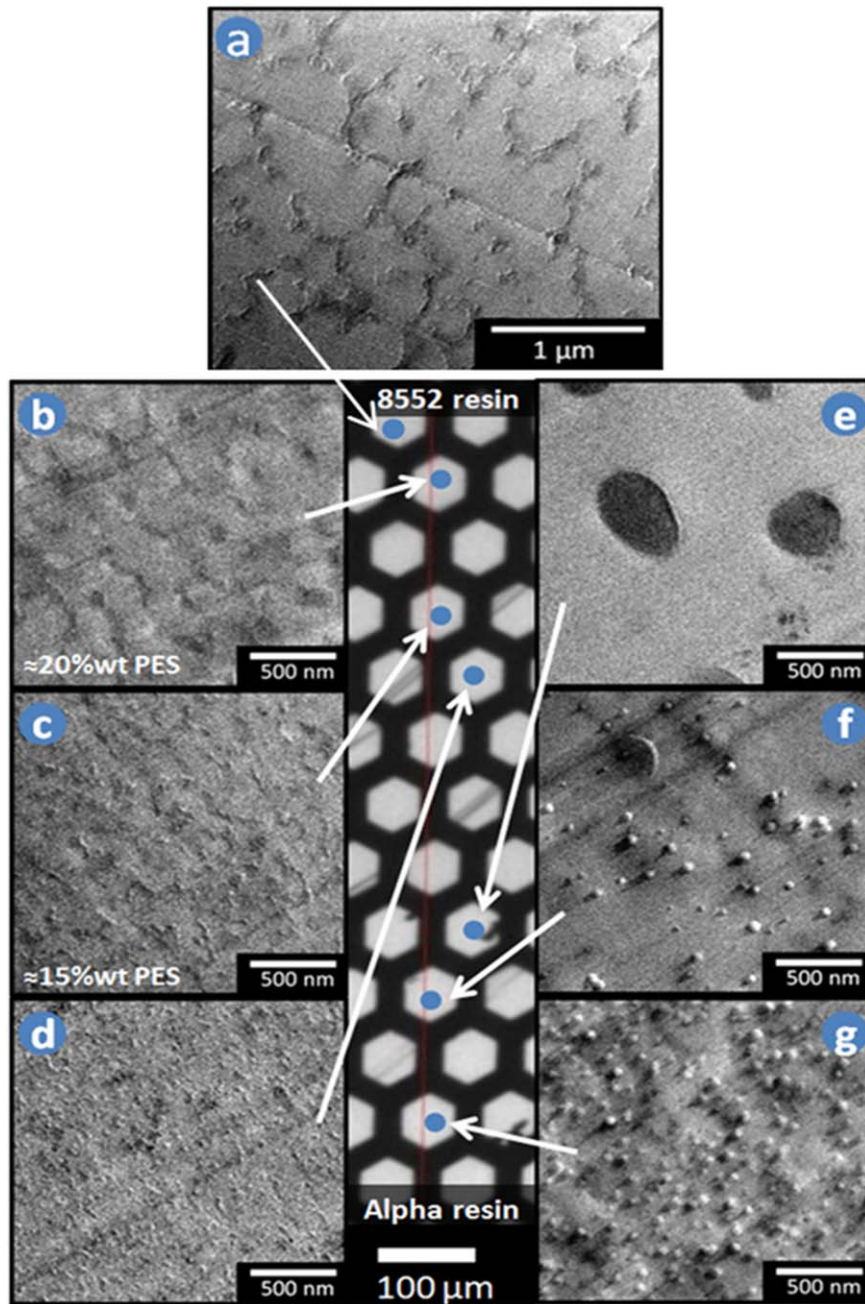


FIG. 5. (a) Low magnification TEM image of ultrathin section of “Model 1” sample supported on a TEM grid in the interfacial region between 8552 and alpha resin (composition gradient is in the vertical direction); (b–g) high magnification TEM micrographs of interfacial gradient zones from pure 8552 (b) to pure alpha (g) resins and intermediate compositions across the interphase (c–f). [Color figure can be viewed in the online issue, which is available at [wileyonlinelibrary.com](http://wileyonlinelibrary.com).]

tightness. The presence of carbon fibers limits the diffusion of the 8552 resin to about  $150\ \mu\text{m}$  into the alpha resin. On the other hand, as can be observed in Fig. 4b, the alpha resin diffusion through the 8552 prepreg is less hampered because of its low viscosity and slower crosslinking kinetics (see Table 1). The combined effects produce different penetration depths for the two resins and lead to a non-symmetric profile.

The investigation of the microstructure gradient across the interphase is another way to estimate the interdiffusion distance.

Figure 5a and g presents TEM micrographs of the neat 8552 and alpha resins. The corresponding microstructures can be considered as the boundaries for the interdiffusion zones.

The 8552 resin contains 20% wt PES, which acts as toughener. Upon curing, the PES phase-separates from the epoxy component by reaction induced phase separation (RIPS) and the system exhibits a morphology close to co-continuity see Fig. 5a. On the other hand, the alpha resin shows a homogenous distribution of individual spherical nano-inclusions with about 50 nm

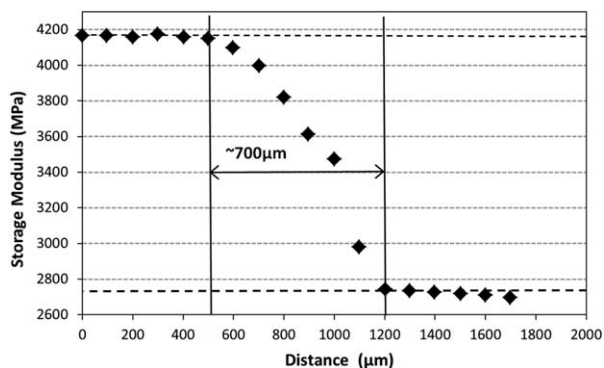


FIG. 6. Modulus evolution in the 8552-alpha resin interphase.

diameter size, see Fig. 5g. This morphology is similar to the one observed in nanosilica-modified prepreps [28] or in epoxy resins toughened with core-shell-rubber particles [29]. The nanoparticles act as tracers of the alpha resin and can be used to follow the interdiffusion profile.

Depending on the thermoplastic content of an epoxy-thermoplastic blend, the microstructure after RIPS evolves from a sea-island morphology with thermoplastic droplets dispersed in a continuous epoxy-rich phase at low thermoplastic concentration to a phase inverted morphology with epoxy inclusions dispersed in a continuous thermoplastic-rich phase at high thermoplastic concentration. The transition between these two morphologies is characterized by a co-continuous structure [30]. In the case of the 8552-alpha resin system, the TEM micrographs show a complex morphology gradient in the interdiffusion zone which results from the mixing of both resin precursors. As shown in Fig. 5, the microtomes are placed on a TEM grid with a mesh design allowing to follow the microstructure evolution across the interphase. These observations, though qualitative, provide an additional estimate of the interdiffusion distance. Between the boundaries corresponding to the neat 8552 and alpha resins, the local composition constantly evolves across the interphase, leading to a microstructure gradient, as can be observed in Fig. 5a–g. The evolution of both the PES microstructure and the alpha resin tracer nanoparticles guides the analysis of the morphology.

The co-continuous morphology progressively evolves into a sea-island structure with dispersed thermoplastic nodules in a continuous epoxy resin-rich phase when moving to the alpha resin side, as observed in Fig. 5c–e. According to studies of similar epoxy-PES blends, phase inversion occurs at around 15 wt% PES [31, 32]. Morphologies corresponding to phase inversion are observed in the region shown in Fig. 5c. On the alpha resin-rich side shown in Fig. 5g, the distribution of nanoparticles is observed. Moving toward the interphase, the concentration of nanoparticles decreases while PES nodules become visible, see Fig. 5f. The microstructure gradient across the interphase obviously results from the concentration gradient due to the interdiffusion between the resins. The estimated size of interdiffusion region is approximately equal to 450–750 μm close to the values inferred by Raman spectroscopy and EDX analysis.

In addition to the evaluation of the concentration profiles and of the morphology gradient, the evolution of the local modulus across the interphase is determined by nano-indentation. This method has already been used in the literature to determine the

Young's modulus of two neat resins in an infusion-prepreg system [27]. The two resins comprising the model system without carbon fiber have distinct moduli which correspond to the extreme levels of the modulus reported in Fig. 6. The width of the transition zone between the upper and lower limits is estimated to be around 900 μm with one standard deviation added to the measured modulus, as applied above for the Raman and EDX estimates.

The previous analyses performed by Raman spectroscopy, SEM-EDX, TEM, and nano-indentation on independent samples reveal a consistent interdiffusion distance of about 700–900 μm for model systems in the absence of carbon fibers. In order to quantitatively compare results from Raman spectroscopy and nano-indentation, both measurements are performed on the same sample and at the same location across the interphase. The resulting quantitative profiles illustrated in Fig. 7 confirm the consistency of the interdiffusion distance estimates. The fact that the elastic modulus evolves with the proportion of resin (i.e., following a simple law of mixture) indicates that it is primarily dominated by the intrinsic molecular structure and cross-linking density more than by the mesoscale microstructure.

Finally, the SEM-EDX profile from Fig. 4a is compared to the Raman from Fig. 3c and nano-indentation profiles from Fig. 6 by arbitrarily superimposing the points corresponding to the 50%/50% mixture from the SEM-EDX and Raman profiles. The TEM micrographs from Fig. 5a–g were also added to Fig. 6 by associating each micrograph to its estimated PES concentration calculated above. The coherence between all the methods is conspicuous.

Figure 8a shows a macroscopic picture of the surface of an SQ-RTM composite made from an 8552 prepreg and alpha injection resin, corresponding to the model systems studied above (see experimental section for details). The colored injection resin clearly appears as pools at locations where the CF tapes do not touch the top surface. There is no evidence of convective motion of the tapes, highlighting the predominance of the interdiffusion during molding.

An EDX analysis is performed across the composite by tracing the sulfur element from the 8552 prepreg and the chlorine element from the alpha resin. The relative concentrations of carbon, sulfur, and chlorine atoms are calculated along a straight line in the thickness direction from the top (zone containing thin film of alpha resin) to the bottom (prepreg rich zone) at each point noted by a yellow cross (Fig. 8b).

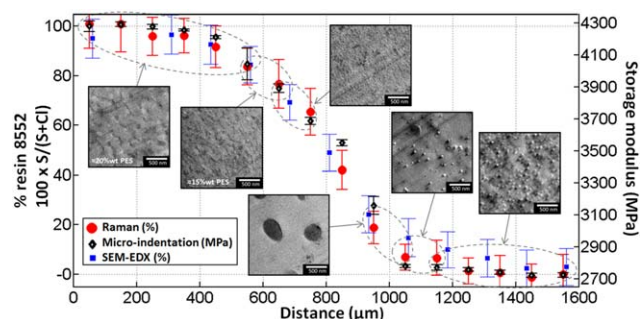


FIG. 7. Comparison between Raman, SEM-EDX, and micro-indentation profiles for an 8552-Alpha resin sample with the associated TEM microstructures. [Color figure can be viewed in the online issue, which is available at [wileyonlinelibrary.com](http://wileyonlinelibrary.com).]

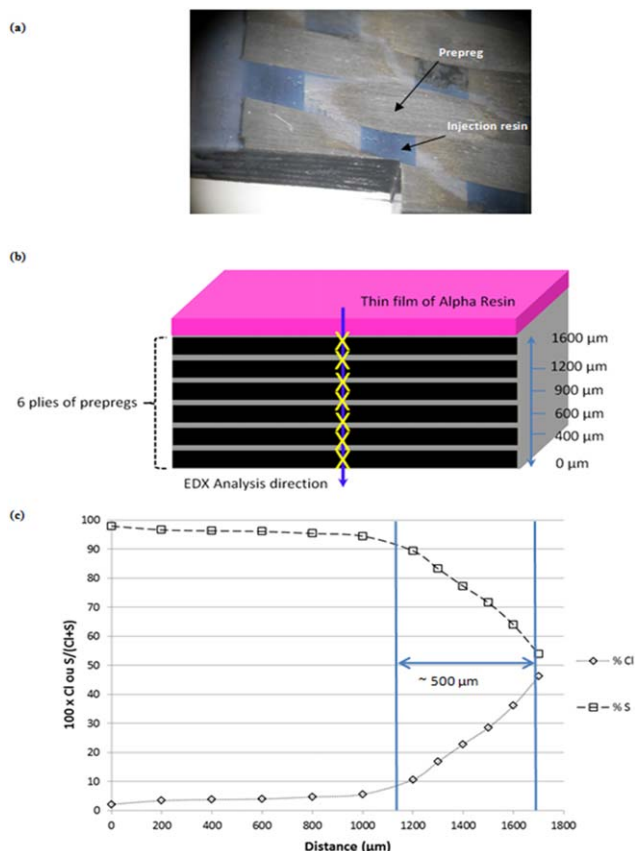


FIG. 8. (a) Micrograph of an SQ-RTM composite showing the injection and prepreg resins, (b) Schematic view of SQ-RTM composite cross-section containing the alpha resin/prepreg 8552, and (c) Percentage of sulfur and chlorine atoms from 8552 and alpha resin respectively through the composite cross-section. [Color figure can be viewed in the online issue, which is available at [wileyonlinelibrary.com](http://www.interscience.wiley.com).]

The 8552 resin mass concentration is defined as  $[100 \times \text{sulfur} / (\text{sulfur} + \text{chlorine})]$ .

Figure 8c shows the interdiffusion profile inside the composite sample. An interdiffusion distance of  $\sim 500 \mu\text{m}$  can be estimated, indicating that the alpha resin diffuses throughout approximately 2 plies of prepreps, which is similar to the results obtained on the Model System 2 with carbon fibers.

The results for the model and real SQ-RTM systems confirm that interdiffusion is an essential element to be considered for the fine-tuning of this process. The measurements made on the model system match the real composite case pretty well, which is important in view of the optimization of SQ-RTM in terms of the selection of the best couples of resins.

## CONCLUSIONS

Model systems were processed under representative conditions of the local environment found at the periphery of composite panels produced by the novel “Same Qualified-Resin Transfer Molding” process. The interdiffusion and the resulting interfacial profile between a realistic couple of prepreg and injection resins used with this process were studied using Raman spectroscopy coupled with chemometrics, X-ray spectrometry coupled with scanning electron microscopy, transmission electron microscopy, and nano-indentation. An interdiffusion distance around 700–900

$\mu\text{m}$  was consistently estimated with the four different techniques for the neat resin systems and confirmed by replicate samples. Moreover, some asymmetry was observed in the interdiffusion profile, with the low viscous resin diffusing further than the high viscous one. SEM-EDX enabled the analysis of samples containing carbon fibers and showed that the presence of the fibers limits the interdiffusion to 500  $\mu\text{m}$ . This distance is significant when compared to the thickness of typical composite panels and of single plies. The results obtained on the model systems match very well with the interdiffusion profiles obtained on real SQ-RTM composites processed with the same resin combination.

## ACKNOWLEDGMENT

The authors gratefully thank ECOTAC partners (SONACA, SABCA and Techspace aero. . .), UCL/IMCN/BSMA collaborators and UCL/iMMC/IMAP coworkers.

## REFERENCES

1. M. Wallin, O. Saarela, L. Barnaby, and T. Liehu, “RTM Composite Lugs for High Load Transfer Applications,” in ICAS 2006—25th International Congress of the Aeronautical Sciences, Hamburg, Germany.
2. K. Mason, “Autoclave Quality Outside the Autoclave,” in High-Performance Composite, (2006). Available at: <http://www.compositesworld.com/articles/autoclave-quality-outside-the-autoclave>.
3. S. Black, “SQRTM Enables Net-Shape Parts” in High-Performance Composite, (2010). Available at: <http://www.compositesworld.com/articles/sqrtm-enables-net-shape-parts>.
4. C.D. Fratta, M. Danzi, V. Gabathuler, M. Zogg, and P. Ermanni, *Sample J.*, **48**, 40 (2012).
5. C. Wellhausen, R. Schulze, H. Wehlan, S. Kunze, K. Drechsler, and K. Horn, “Morphology Analysis of Epoxy Matrices to Determine Resin Interface Zones Within Combined Prepreg and Infusion Processing,” in erschienen 2009 Proceeding: EUCOMAS, Augsburg, Germany (2009).
6. S. Eibl, *J. Compos. Mater.*, **42**, 1231 (2008).
7. Hexcel Composites Ltd, *Safety Data Sheet HexPly 8552 Resin*, Duxford, Cambridge, UK.
8. Hexcel Composites SA, Safety Data Sheet “Alpha resin”, Z.I. La Plaine, Montluel, France.
9. K. Mimura, H. Ito, and H. Fujioka, *Polymer*, **41**, 2385 (2000).
10. M.A. Andrés, J. Garmendia, A. Valea, A. Eceiza, and I. Mondragon, *Appl. Polym. Sci.*, **69**, 183 (1998).
11. E. Van Overbeke, J. Devaux, R. Legras, J.T. Carter, P.T. McGrail, and V. Carlier, *Appl. Spectrosc.*, **55**, 540 (2001).
12. E. Van Overbeke, J. Devaux, R. Legras, J.T. Carter, P.T. McGrail, and V. Carlier, *Appl. Spectrosc.*, **55**, 1514 (2001).
13. J.F. Aust, K.S. Booksh, C.M. Stellman, R.S. Parnas, and M.L. Myrick, *Appl. Spectrosc.*, **51**, 247 (1997).
14. H. Martens, T. Naes, *Multivariation Calibration*, Wiley. Chichester, UK (1989).
15. K. Dittmar, H.W. Siesler, and J. Fresenius, *Anal. Chem.*, **362**, 109 (1998).
16. R.E. Aries, J. Sellors, and R.A. Spragg, “Principal Components Analysis for FTIR Spatial Mapping and Time Resolved Data, in” *Analytical Applications of Spectroscopy II*, A.M.C. Davies and C.S. Creaser, Eds., RCS, Cambridge, UK, p 248 (1998).

17. L.J. Vandi, M. Hou, M. Veidt, R. Truss, M. Heitzmann, R. Paton, "Interface Diffusion and Morphology of Aerospace Grade Epoxy Co-cured with Thermoplastic Polymers," in ICAS, Brisbane, Australia, 2012.
18. P.J.M. Van Espen, and K.H.A. Jansen, in *Handbook of X-Ray Spectrometry*, Eds., R.E. Van Grieken and A.A. Markowicz, M. Decker Inc, New York, Editon edn., 181 (1993).
19. J. Osán, J. De Hoog, P. Van Espen, I. Szalóki, C.U. Ro, and R. Van Grieken, *X-ray Spectrom.*, **30**, 419 (2001).
20. T. Kyotani, *Bull. Chem. Soc. Jpn.*, **74**, 723 (2001).
21. G. Boon and G. Bastin, *Microchim. Acta*, **147**, 125 (2004).
22. G.F. Bastin, J.M. Dijkstra, and H.J.M. Heijligers, *X-ray Spectrom.*, **27**, 3 (1998).
23. X. Li and B. Bhushan, *Mater. Character.*, **48**, 1 (2002).
24. L. Cheng, X. Xia, W. Yu, L.E. Scriven, and W.W. Gerberich, *J. Polym. Sci. Part B: Polym. Phys.*, **38**, 10 (2000).
25. J.H. Gwynne, M.L. Oyen, and R.E. Cameron, *Polym. Test.*, **29**, 494 (2010).
26. E. Van Overbeke, J. Devaux, R. Legras, J.T. Carter, P.T. McGrail and V. Carlier, *Polymer*, **44**, 4899 (2003).
27. R. Kaps and M. Wiedemann, "Combined Prepreg and Resin Infusion Technologies: Novel Integral Manufacturing Processes for Cost-Efficient CFRP Components," in *Adaptive, Tolerant and Efficient Composite Structures*, Springer-Verlag, Berlin Heidelberg, 349 (2013).
28. C. Aitken and Q. Pham, *Sampe J.*, **49**, 7 (2013).
29. M. Nobuo, *JEC Compos. Mag.*, **79**, 85 (2013).
30. C.B. Bucknall and I.K. Partridge, *Polymer*, **24**, 638 (1983).
31. D. Dumont, Doctoral Thesis, EPL UCL, 68 (2012).
32. P. Van Velthem, W. Ballout, D. Daoust, M. Slavons, F. Cordenier, E. Henry, D. Dumont, V. Destoop, T. Pardoën, and C. Bailly, *Compos. A*, **72**, 175 (2015).